Available online at www.sciencedirect.com
ScienceDirect
Journal of Nutritional Biochemistry 20 (2009) 663–676
Journal of Nutritional Biochemistry

RESEARCH ARTICLES

Isoliquiritigenin inhibits migration and invasion of prostate cancer cells: possible mediation by decreased JNK/AP-1 signaling☆

Gyoo Taik Kwon[a,1], Han Jin Cho[a,1], Won-Yoon Chung[b], Kwang-Kyun Park[b], Aree Moon[c], Jung Han Yoon Park[a,*]

[a]Department of Food Science and Nutrition, Hallym University, Chuncheon, 200-702, South Korea
[b]Department of Oral Biology, College of Dentistry, Yonsei University, Seoul, 120-752, South Korea
[c]College of Pharmacy, Duksung Women's University, Seoul, 132-714, South Korea

Received 29 January 2008; received in revised form 24 May 2008; accepted 9 June 2008

Abstract

Isoliquiritigenin (ISL, 4,2′,4′-trihydroxychalcone), which is found in licorice, shallot and bean sprouts, is a potent antioxidant with anti-inflammatory and anti-carcinogenic effects. The purpose of this study was to investigate the effects of ISL treatment on the migration, invasion and adhesion characteristics of DU145 human prostate cancer cells. DU145 cells were cultured in the presence of 0–20 μmol/L ISL with or without 10 μg/L epidermal growth factor (EGF). ISL inhibited basal and EGF-induced cell migration, invasion and adhesion dose dependently. ISL decreased EGF-induced secretion of urokinase-type plasminogen activator (uPA), matrix metalloproteinase (MMP)-9, tissue inhibitor of metalloproteinase-1 (TIMP-1), and vascular endothelial growth factor (VEGF), but increased TIMP-2 secretion in a concentration-dependent manner. In addition, ISL decreased the protein levels of integrin-α2, intercellular adhesion molecule (ICAM) and vascular cell adhesion molecule (VCAM), and mRNA levels of uPA, MMP-9, VEGF, ICAM and integrin-α2. Furthermore, basal and EGF-induced activator protein (AP)-1 binding activity and phosphorylation of Jun N-terminal kinase (JNK), c-Jun and Akt were decreased after ISL treatment. However, phosphorylation of extracellular signal-regulated kinase (ERK)1/2 and p38 mitogen-activated protein kinase was not altered. The JNK inhibitor SP600125 inhibited basal and EGF-induced secretion of uPA, VEGF, MMP-9 and TIMP-1, as well as AP-1 DNA binding activity and cell migration. These results provide evidence for the role of ISL as a potent antimetastatic agent, which can markedly inhibit the metastatic and invasive capacity of prostate cancer cells. The inhibition of JNK/AP-1 signaling may be one of the mechanisms by which ISL inhibits cancer cell invasion and migration.

Keywords: Matrix metalloproteinase; EGF; Tissue inhibitor of metalloproteinase; Activator protein-1; Jun N-terminal kinase

1. Introduction

Chemoprevention of cancer has gained considerable attention recently, probably because it involves the use of dietary bioactive compounds either alone or in combination to reverse, suppress or prevent cancer progression [1]. Epidemiological studies followed by laboratory studies have shown that dietary agents are an important factor in reducing cancer risk [2–4]. Diets rich in naturally occurring polyphenolic flavonoids have been shown to be associated with a reduced incidence of various human cancers [2–5].

Prostate cancer is the second leading cause of cancer-related deaths in men in the US [6], and the incidence of this disease is increasing in both developed and developing countries. Androgen deprivation therapy by either bilateral orchiectomy

Abbreviations: AP-1, activator protein-1; EGF, epidermal growth factor; ERK, extracellular signal-regulated kinase; ICAM, intercellular adhesion molecule; ISL, isoliquiritigenin; JNK, Jun-N-terminal kinase; MAPK, mitogen-activated protein kinase; MMP, matrix metalloproteases; TIMP, tissue inhibitor of metalloproteinase; uPA, urokinase-type plasminogen activator; VCAM, vascular cell adhesion molecule; VEGF, vascular endothelial growth factor.

☆ This work was supported by Basic Research Program of the Korea Science and Engineering Foundation (R01-2004-000-10177-0) and a grant (code number: 20070301034039) from BioGreen 21 Program, Rural Development Administration, Republic of Korea.

* Corresponding author. Tel.: +82 33 248 2134; fax: +82 33 256 0199.
E-mail address: jyoon@hallym.ac.kr (J.H.Y. Park).

[1] The first two authors contributed equally to this work.

0955-2863/$ – see front matter © 2009 Elsevier Inc. All rights reserved.
doi:10.1016/j.jnutbio.2008.06.005

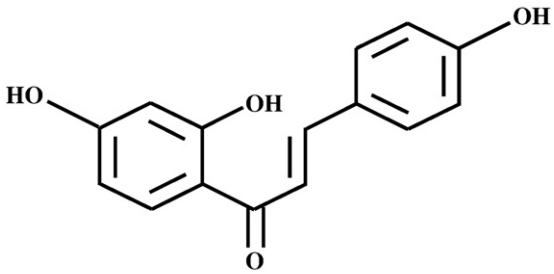

Isoliquiritigenin (ISL)

Fig. 1. Structure of ISL.

or treatment with gonadotrophin-releasing hormone agonist is the mainstay of therapy for advanced prostate cancer. However, androgen ablation therapy eventually fails, and prostate cancer progresses to a hormone-refractory state. Most patients with cancer die not because of the tumor in the original site, but because of the development of metastasis [7]. Therefore, it is important to inhibit the spread of tumor cells, thereby inhibiting the development of metastasis. Accordingly, the anti-metastastic effects of nontoxic dietary agents could be of special significance in the prevention, control and/or management of prostate cancer, especially that at an advanced and an androgen-independent stage of the disease. Many dietary bioactive components have shown promising anti-cancer activities with little or no toxicity to normal cells [8–10]. For that reason, investigations of how dietary bioactive components regulate adhesion, invasion and motility of cancer cells could play a significant role in the development of new agents with low toxicity to prevent and treat cancer.

Isoliquiritigenin (ISL, Fig. 1) is a flavonoid belonging to the chalcone family that is found in licorice, shallot and bean sprouts. ISL has been reported to inhibit 7,12-dimethylbenz [α]anthracene-initiated and 12-*O*-tetradecanoyl-phorbol-13-acetate-promoted skin papilloma formation [11], induction of aberrant crypt foci and colon carcinoma development in azoxymethane-treated ddY mice [12] and pulmonary metastasis of mouse renal cell carcinoma [13]. We and other investigators have reported that ISL inhibits cell growth and ErbB3 signaling, and induces apoptosis in prostate cancer cells [14–16]. However, the effects of ISL on metastasis of prostate cancer and the mechanisms underlying these effects have not been studied. The present study was performed to examine whether ISL inhibits adhesion, invasion and motility of prostate cancer cells. We demonstrated that ISL potently inhibits the metastastic potential of DU145 human prostate cancer cells, an effect which may be mediated through inhibition of Jun N-terminal kinase (JNK)/AP-1 signaling.

2. Materials and methods

2.1. Materials

The following reagents were purchased from the indicated suppliers. ISL and SP600125, an inhibitor of JNK [17], Sigma (St. Louis, MO, USA); antibodies against Akt, JNK, extracellular signal-regulated kinase (ERK)1/2, p38 mitogen activated protein kinase (MAPK) and c-Jun, Cell Signaling (Beverly, MA, USA); antibodies against matrix metalloproteases (MMP)-9, integrin-α2, tissue inhibitor of metalloproteinase-1 (TIMP-1), TIMP-2, intercellular adhesion molecule (ICAM), vascular cell adhesion molecule (VCAM) and vascular endothelial growth factor (VEGF), Santa Cruz Biotechnology, Inc. (Santa Cruz, CA, USA); anti-urokinase-type plasminogen activator (uPA), Calbiochem (Darmstadt, Germany); VEGF enzyme-linked immunosorbent assay (ELISA) kit and epidermal growth factor (EGF), R&D systems (Minneapolis, MN, USA); matrigel invasion chambers, BD Biosciences (San Jose, CA, USA); adhesion assay kit and Centricon Plus-20, Millipore Corporation (Billerica, MA, USA). If not denoted differently, all other materials were obtained from Sigma.

2.2. Cell culture and cell viability assay

PWR-1E normal prostate epithelial cells, androgen-sensitive LNCaP and androgen-independent DU145 prostate cancer cells, and HT1080 human fibrosarcoma cells were obtained from American Type Culture Collection (Manassas, VA, USA). LNCaP and DU145 cells were maintained in DMEM/F12, containing 100 ml/L fetal bovine serum (FBS), with 100,000 U/L penicillin and 100 mg/L streptomycin (Gibco BRL, Gaithersburg, MD, USA). PWR-1E cells were maintained with keratinocyte-serum free medium supplemented with 10% FBS, 5 μg/L EGF and 0.05 g/L bovine pituitary extract (Invitrogen, Carlsbad, CA, USA). To examine the effect of ISL on PWR-1E cells, the cell monolayers were rinsed and serum deprived for 24 h, using keratinocyte-serum free medium supplemented with 1% charcoal-stripped FBS, 5 μg/L EGF and 0.05 g/L bovine pituitary extract (serum-deprivation medium). After serum deprivation, the medium was replaced with the fresh serum-deprivation medium with the addition of various concentrations of ISL. The medium was changed every 2 days. Viable cell numbers were estimated by the MTT assay as previously described [18]. ISL was dissolved in dimethyl sulfoxide (DMSO), and all cells were treated with DMSO at a final concentration of 0.02%.

2.3. Migration, invasion and adhesion assays

For the Transwell migration assay, DU145 cells were serum deprived in DMEM/F12 supplemented with 1% charcoal-stripped FBS for 24 h. They were plated onto the filter in 6.5-mm Transwell inserts in 24-well plates at 2.5×10^4 cells/filter and treated with various concentrations of ISL. Prior to plating cells, the lower side of the Transwell filter had been precoated with 10 μg Type IV collagen. The lower chamber of the well was filled with DMEM/F12 containing 1% charcoal-stripped FBS and 0.1% BSA with or without 10 μg/L EGF, 10 nmol/L insulin-like growth factor (IGF)-I or 20 μg/L heregulin (HRG)-β. Cells were incubated

for 4 h. Migrated cells were stained with hematoxylin and eosin (H&E). For LNCaP cells, the serum-deprivation medium was DMEM/F12 plus 5% charcoal-stripped FBS and 1 nmol/L 4,5α-dihydrotestosterone (DHT), and the chemoattractant medium was DMEM/F12 plus 0.1% BSA, 5% charcoal-stripped FBS, 1 nmol/L DHT and 10 μg/L EGF.

For the invasion assay, the same procedures were performed as described in the migration assay except that cells were plated on a matrigel-coated Transwell filter (Matrigel invasion chamber, BD Biosciences).

For the wound migration assay, DU145 cells were plated in six-well plates at 8×10^5 cells/well in DMEM/F12 supplemented with 10% FBS. One day later, the monolayers were serum deprived in DMEM/F12 supplemented with 1% charcoal-stripped FBS for 24 h. Ninety percent confluent cells were incubated with 1 mg/L mitomycin C in DMEM/F12 containing 1% charcoal-stripped FBS for 1 h. After mitomycin C treatment, the injury line was made with a yellow tip and rinsed with PBS. The cells were then incubated with 0 μmol/L ISL, 20 μmol/L ISL, 10 μg/L EGF or 10 μg/L EGF+20 μmol/L ISL in DMEM/F12 containing 1% charcoal-stripped FBS for 0, 6, 12 or 24 h. Cell migration was observed by microscopy at the indicated time points. The measured width of injury lines was plotted as a percentage of the width at 0 h.

For the adhesion assay, DU145 cells were plated in human collagen Type I-coated CytoMatrix Cell Adhesion Strips. Cells were incubated in DMEM/F12 containing 1% charcoal-stripped FBS with 0–20 μmol/L ISL with or without 10 μg/L EGF for 45 min. Strips were rinsed twice with PBS (containing Ca^{2+}/Mg^{2+}) and stained for 5 min with 0.2% crystal violet in 10% ethanol. After staining, the cell-bound stains were quantified by determining the absorbance at 570 nm on a microplate reader.

2.4. Gelatin zymography

Cells were serum starved in DMEM/F12 and treated with 10 μg/L EGF for 48 h in the absence or presence of ISL. Conditioned media were collected and concentrated by centrifugal ultrafiltration using Centricon Plus-20 with a molecular exclusion of 10,000. Proteins in conditioned media were separated by SDS-PAGE. The volumes of media loaded onto the gel were adjusted for equivalent protein levels. After electrophoresis, the gels were washed twice in 2.5% Triton X-100 for 30 min to eliminate SDS completely. The gels were then rinsed twice with zymogen activation buffer (50 mmol/L Tris-HCl, 0.02% Brij 35, 5 mmol/L $CaCl_2$ and 0.2 mmol/L NaCl) and were incubated for 48 h at 37°C in the same buffer. After incubation, the gels were stained for 2 h with 0.25% Commassie Blue solution and destained.

2.5. Western blot analyses and VEGF ELISA

Cells were lysed as described previously [19], and the protein contents determined using a BCA protein assay kit (Pierce, Rockford, IL, USA). The total cell lysates (50 μg protein) and concentrated conditioned media were resolved on SDS-PAGE (4–20% or 10–20%) and transferred onto a polyvinylidene fluoride membrane (Millipore, Billerica, MA). The blots were blocked for 1 h with 50 g/L nonfat dry milk dissolved in 20 mmol/L Tris-HCl, pH 7.5, 150 mmol/L NaCl and 0.1% Tween 20, and then incubated for 1 h with individual primary antibodies. The blots were then incubated with anti-mouse, goat or rabbit HRP-conjugated antibody. Signals were detected via enhanced chemiluminescence, using SuperSignal West Dura Extended Duration Substrate (Pierce). Densitometric analyses were conducted using the Bio-profile Bio-ID application (Vilber-Lourmat, France). The expression levels were normalized to β-actin, and the control levels were set to 100%. The levels of VEGF in conditioned media were also estimated by the VEGF ELISA kit (R&D System) according to the manufacturer's instruction.

2.6. Reverse transcription-PCR

Total RNA was isolated with Tri reagent (Sigma), and the cDNA was synthesized using 3 μg of total RNA and SuperScript II reverse transcriptase (Invitrogen, Carlsbad, CA, USA), as described previously [20]. The cDNA was amplified in accordance with the previously described procedure [21]. Sequences for PCR primer sets, annealing temperatures and numbers of cycles used for PCR amplification are listed in Table 1. For each combination of primers, the PCR amplification kinetics was determined, the number of cycles corresponding to the plateau was counted and PCR was conducted within an exponential range. The PCR products were separated on 1% agarose gel

Table 1
Primer sequences used for PCR amplification

mRNA	Primer sequences	Annealing temperature	Number of cycle
MMP-9	Sense: TTC ATC TTC CAA GGC CAA TC Anti-sense: CTT GTC GCT GTC AAA GTT CG	60	31
uPA	Sense: AGA ATT CAC CAC CAT CGA GA Anti-sense: ATC AGC TTC ACA ACA GTC AT	48	25
Integrin-α2	Sense: GAC GTG CTC TTG GTA GGT GCA Anti-sense: GAC CAG AGT TGA ACC ACT TG	54	35
ICAM	Sense: GGT GAC GCT GAA TGG GGT TCC Anti-sense: GTC CTC ATG GTG GGG CTA TG	55	25
VEGF	Sense: AGG AGG GCA GAA TCA TCA CG Anti-sense: CAA GGC CCA CAG GGA TTT TCT	55	24
β-actin	Sense: GTT TGA GAC CTT CAA CAC CCC Anti-sense: GTG GCC ATC TCC TGC TCG AAG TC	60	27

and stained with ethidium bromide. Bands corresponding to each of the specific PCR products were quantitated via the densitometric scanning of the exposed film, using the Bio-profile Bio-ID application. The mRNA levels were normalized to β-actin, with the control level set to 100%.

2.7. Preparation of nuclear extract

DU145 cells were washed briefly with ice-cold PBS containing 1 mmol/L iodoacetic acid and 1 mmol/L PMSF, then lysed with hypotonic buffer (10 mmol/L HEPES, pH 7.9, 1.5 mmol/L $MgCl_2$, 10 mmol/L KCl, 0.2 mmol/L PMSF, 0.5 mmol/L DTT, 5 mL/L NP-40, 10 mmol/L iodoacetic acid, 20 mg/L aprotinin, 10 mg/L antipain, 10 mg/L leupeptin, 80 mg/L benzamidine HCl) on ice for 10 min. After centrifugation (2300×*g* for 15 min at 4°C), pellets were resuspended with hypotonic buffer (without NP-40). The nuclei were pelleted by centrifugation and resuspended in 150-μl low salt buffer (20 mmol/L HEPES, pH 7.9, 1.5 mmol/L $MgCl_2$, 10 mmol/L KCl, 0.2 mmol/L PMSF, 0.2 mmol/L EDTA, 0.5 mmol/L DTT, 100 mL/L glycerol). Fifty-microliter high salt buffer (containing 1.6 mol/L KCl) was then added dropwise, and the mixture was incubated for 1 h on ice. After centrifugation (25,000×*g* for 30 min at 4°C), the supernatant was retained for use in the DNA binding assay.

2.8. Electrophoretic mobility shift assay

Double-stranded DNA probes for AP-1 (5′-CGC TTG ATG AGT CAG CCG GAA-3′) were used for electrophoretic mobility shift assay (EMSA) after end-labeling of the probe with [γ-^{32}P]ATP and T4 kinase. Nuclear extracts (10 μg) were incubated in 30-μl binding buffer (10 mmol/L Tris-HCl, 100 mmol/L NaCl, 1 mmol/L EDTA, 4% glycerol, 1 mmol/L DTT) and 1 μg poly(dIdC) for 30 min at 37°C. For competitive experiments, nuclear extracts were preincubated with a 20-fold molar excess of unlabeled probe for 15 min. Each sample was subjected to 5% nondenaturing gel, and the gels were dried and visualized by autoradiography.

2.9. Statistical analysis

The results were expressed as means±S.E.M. and analyzed via ANOVA. Differences among the treatment groups were assessed by Duncan's multiple range test, using the SAS system for Windows v. 8.1.

3. Results

3.1. EGF, and not IGF-I or heregulin-β, induces migration of DU145 cells

Since it has been reported that the androgen-independent human prostate cancer cell line DU145 and the androgen-sensitive prostate cancer cell line LNCaP are responsive to stimulation with EGF and IGF-I [22], we first examined whether IGF-I, heregulin-β or EGF stimulates cell migration and MMP secretion in DU145 cells. The Transwell migration assay revealed that EGF markedly increased

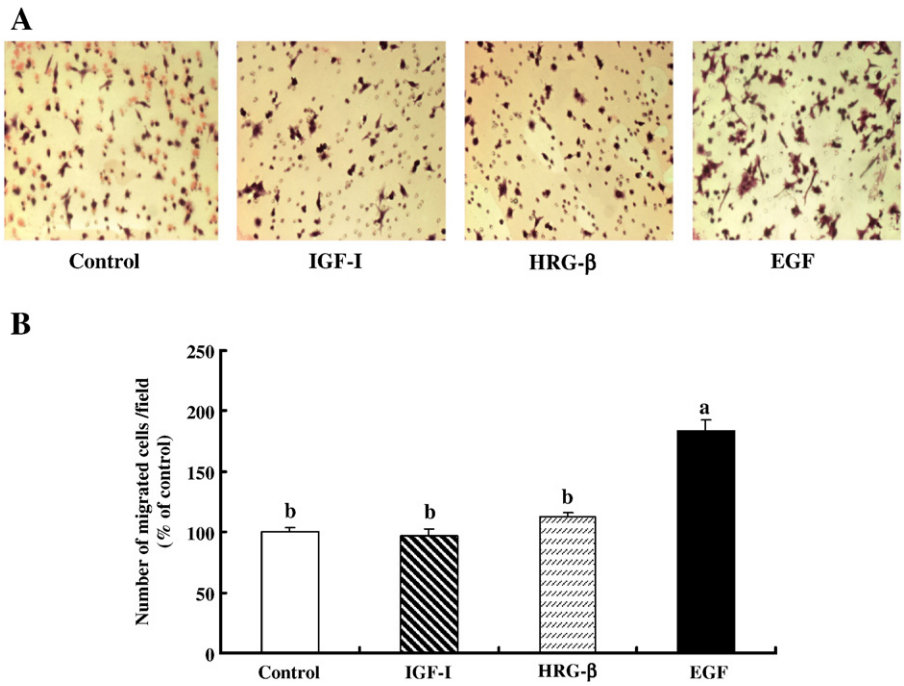

Fig. 2. EGF, but not IGF-1 or HRG-β, induces migration of DU145 cells. The migration of DU145 cells through a Type IV collagen-coated Transwell filter was assessed with 10 μg/L EGF, 10 nmol/L IGF-I or 20 μg/L HRG-β. Cells were incubated for 4 h. (A) Photographs of migrated H&E-stained cells are shown (×100). (B) Quantitative analysis of the migrated cells. Each bar represents the mean±S.E.M. (n=3). Means without a common letter differ (P<.05).

DU145 cell migration, whereas neither IGF-I nor heregulin had any effect on cell migration (Fig. 2). Gelatin zymography results revealed that EGF increased MMP-9 secretion, but neither IGF-I nor heregulin-β had any effect (data not shown).

The cytotoxic effects of ISL on PWR-1E normal prostate epithelial cells were evaluated using the MTT assay. As the viability of PWR-1E cells was not significantly affected by ISL up to 20 μmol/L (data not shown), we chose a concentration of 5–20 μmol/L ISL for the subsequent experiments.

3.2. Isoliquiritigenin inhibits migration and invasion of prostate cancer cells

As EGF stimulated DU145 cell migration, we cultured cells in the absence or presence of EGF to examine whether ISL inhibits cell migration and invasion of DU145 cells. The wound (Fig. 3) and Transwell (Fig. 4A) migration assays revealed that ISL significantly inhibited both basal and EGF-induced migration of DU145 cells. ISL also inhibited basal and EGF-induced migration of androgen-sensitive LNCaP cells (Fig. 4B). Because we previously observed that treatment of DU145 cells with 20 μmol/L ISL for 48 h led to apoptosis [14], the Transwell filter migration assay was performed for 4 h to minimize the contribution of apoptosis. In addition, the wound migration assay was carried out in the presence of mitomycin C to eliminate the contribution of proliferation. The Transwell invasion assay was also performed using matrigel-coated filter, which showed that ISL inhibited basal and EGF-stimulated invasion of DU145 cells (Fig. 4C). The inhibition of EGF-induced cell migration and invasion was ISL dose dependent at concentrations of 5, 10 and 20 μmol/L.

Since proteolytic cleavage of the extracellular matrix (ECM) proteins is a necessary step in the invasion of cancer cells, we next examined the effect of ISL on secretion of MMPs, uPA and TIMPs. Gelatin zymography of serum-free DU145 cell conditioned media revealed the presence of three size classes of MMPs (Fig. 5A): a doublet of bands migrating in the 82,000 to 92,000 M_r range, and two bands at 72,000 and 45,000 M_r. The 92,000- and

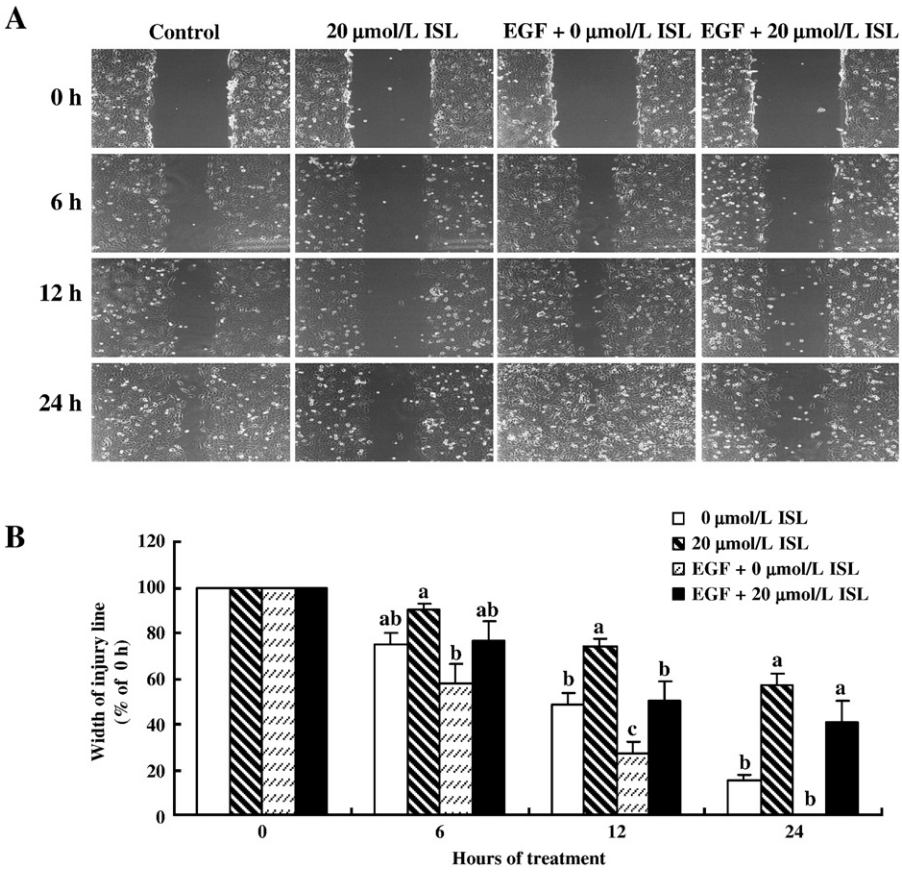

Fig. 3. ISL decreases migration of DU145 cells — Wound migration assay. Ninety percent confluent DU145 cells were treated with 1 mg/L mitomycin C, and the injury line was made with a tip. The cells were then incubated with or without 20 μmol/L ISL in the absence or presence of 10 μg/L EGF in DMEM/F12 containing 1% charcoal-stripped FBS for 0, 6, 12 or 24 h. (A) Cell migration was observed by microscopy at the indicated time points (×40). (B) The measured width of injury lines was plotted as a percentage of the width at 0 h. Each bar represents the mean±S.E.M. (n=3). Means at a time without a common letter differ (P<.05).

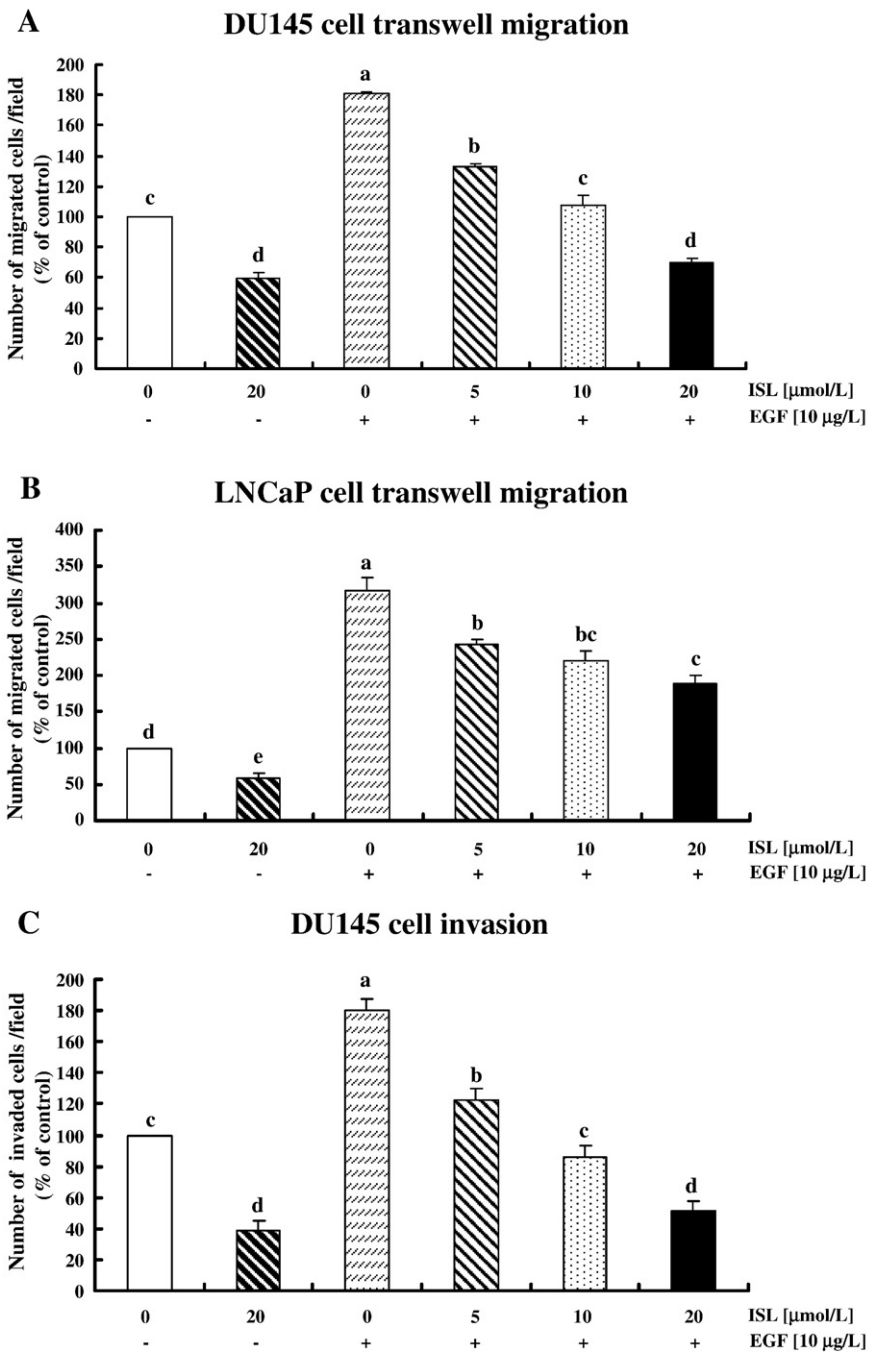

Fig. 4. ISL decreases migration and invasion of prostate cancer cells — Transwell filter migration and invasion assays. The migration of DU145 (A) and LNCaP (B) cells through a Type IV collagen coated filter was performed as described in Fig. 2. (C) DU145 cell invasion was measured with the same procedure described in Fig. 2 except that a matrigel-coated Transwell filter was used. The migrated (A, B) or invaded cells (C) were quantified by counting of H&E-stained cells. Each bar represents the mean±S.E.M. (n=3). Means without a common letter differ (P<.05).

72,000-M_r bands comigrated with MMP-9 and MMP-2 produced by HT1080 human fibrosarcoma cells (Fig. 5A, Lane 1). In addition, it has been reported that DU145 cells produce MMP-9 and MMP-2 [23]. EGF-stimulated secretion of both pro- and active MMP-9 and ISL inhibited both basal and EGF-stimulated MMP-9 secretion. However, the levels of pro-MMP-2 were not altered by treatment with either EGF or ISL. A band with an M_r of 45,000 was also detected, the intensity of which was increased by EGF and decreased by ISL (Fig. 5A). It has been reported that active MMP-2 is subject to autolysis which generates the central 45-kDa gelatinolytically active fragment [24]. These results indicate that active MMP-2 was autolysed very quickly in these cells and therefore could not be detected in the

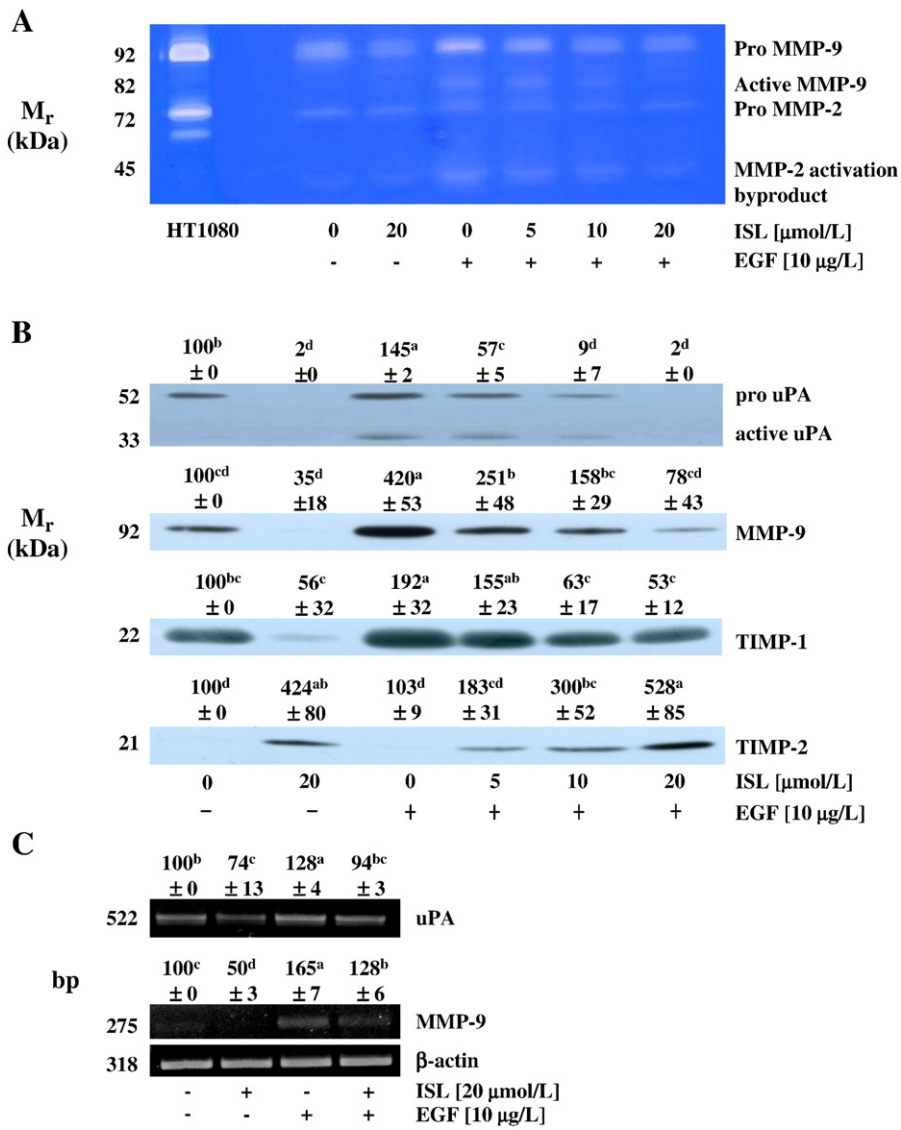

Fig. 5. ISL decreases MMP-9 secretion and increases TIMP-2 secretion in DU145 cells. Serum-starved DU145 cells were incubated with 0–20 μmol/L ISL in DMEM/F12 containing 0 or 10 μg/L EGF for 48 h. Forty-eight-hour conditioned media were collected and concentrated for gelatin zymography (A) and Western blotting (B). The volumes of media loaded onto the gel were adjusted for equivalent protein levels. (C) Serum-starved cells were incubated with ISL and/or EGF for 2 h. Total RNA was isolated for RT-PCR analysis. Photographs of the Commassie blue-stained gel (A), chemiluminescent detection of the blots (B) and ethidium bromide-stained gels (C), which are representative of three independent experiments, are shown. In the first lane of (A), serum-free HT 1080 cell-conditioned medium was loaded. The relative abundance of each band (B) or that to its own β-actin (C) was quantified, and the control levels were set at 100%. The adjusted mean±S.E.M. (n=3) of each band is shown above each blot. Means without a common letter differ (P<.05).

present study. Results of Western blot analysis showed that EGF-stimulated secretion of uPA, MMP-9 and TIMP-1 and ISL inhibited secretion of these proteins regardless of whether the cells were treated with EGF. Secretion of TIMP-2 was not affected by EGF but increased by ISL treatment regardless of EGF treatment (Fig. 5B). Results of RT-PCR revealed that EGF increased the mRNA levels of uPA and MMP-9, and ISL decreased them irrespective of EGF treatment (Fig. 5C).

Results of VEGF ELISA (Fig. 6A) and Western blot analysis (Fig. 6B) showed that ISL inhibited basal and EGF-induced secretion of VEGF by DU145 cells. The levels of VEGF transcripts changed in parallel to those of proteins (Fig. 6C).

3.3. Isoliquiritigenin inhibits adhesion of DU145 cells

The effect of EGF/ISL on adhesion of DU145 cells was estimated using human collagen Type I-coated strips (Fig. 7A). EGF-stimulated DU145 cell adhesion to Type I collagen and ISL inhibited basal and EGF-stimulated cell adhesion. Protein levels of integrin-α2 and ICAM were increased by EGF treatment and decreased by ISL treatment. However, VCAM levels were unaffected by EGF, whereas

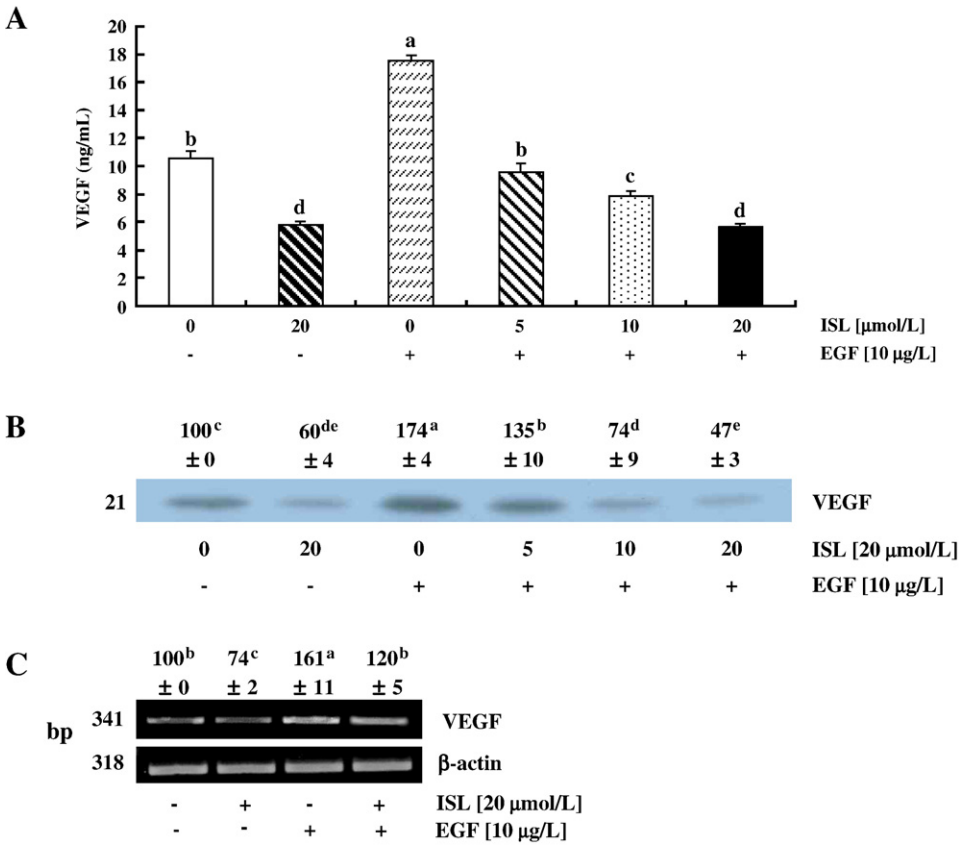

Fig. 6. ISL decreases VEGF secretion. Serum-starved DU145 cells were incubated with 0–20 μmol/L ISL in DMEM/F12 containing 0 or 10 μg/L EGF. Twenty-four-hour conditioned media were collected for VEGF ELISA (A), and 48-h conditioned media were collected for Western blotting (B). Serum-starved cells were incubated with ISL and/or EGF for 2 h. Total RNA was isolated for RT-PCR analysis (C). Each bar represents the mean±S.E.M. (n=4) (A). Photographs of the chemiluminescent detection of the blots (B) and ethidium bromide-stained gels (C), which are representative of three independent experiments, are shown. The relative abundance of each protein band (B) and mRNA band to its own β-actin (C) was quantified, and the control levels were set at 100%. The adjusted mean ±S.E.M. (n=3) of each band is shown above each blot. Means without a common letter differ (P<.05).

they were decreased by ISL treatment (Fig. 7B). RT-PCR analyses revealed that the steady-state levels of integrin-α2 and ICAM transcripts were increased by EGF treatment and decreased by ISL treatment (Fig. 7C).

3.4. Isoliquiritigenin inhibits JNK/AP-1 signaling

EGF binding to the EGF receptor (EGFR) results in receptor dimerization, autophosphorylation and activation of various downstream signaling molecules including phosphatidylinositol-3-kinase (PI3K/Akt) and MAPK [25]. As would be expected, Western blot analyses revealed that treating DU145 cells with EGF led to increased phosphorylation of Akt, p38 MAPK, ERK1/2, JNK and c-Jun. ISL inhibited both basal and EGF-induced phosphorylation of Akt, JNK and c-Jun, but had no effect on phosphorylation of p38 MAPK or ERK1/2 (Fig. 8).

Since ISL inhibited phosphorylation of JNK and c-Jun, we examined next whether the JNK inhibitor SP600125 inhibits DU145 cell migration. Treating cells with 10 μmol/L SP600125 led to a significant decrease in phosphorylation of 54-kDa JNK2 and c-Jun (Fig. 9A). In addition, SP600125 inhibited both basal and EGF-induced secretion of uPA, VEGF, MMP-9 and TIMP-1 (Fig. 9B). Furthermore, the JNK inhibitor significantly inhibited both basal and EGF-induced migration of DU145 cells (Fig. 9C). EGF also stimulated AP-1 DNA binding activity, and ISL and SP600125 inhibited both basal and EGF-induced AP-1 DNA binding activity (Fig. 9D).

4. Discussion

ISL has been reported to have anticarcinogenic effects in both *in vivo* and *in vitro* experimental models. Results from animal studies revealed that ISL inhibits chemically induced colonic tumorigenesis [12], skin papilloma formation [11] and lung metastasis of murine renal cell carcinoma cells [13]. *In vitro* studies showed that ISL has antiproliferation activity in skin [26], pulmonary [13], breast [27] and gastric [28] cancer cells. To date, only three studies have described the antiproliferative effects of ISL on prostate cancer cells [14–16], and the effect of ISL on prostate cancer cell migration or invasion has not been

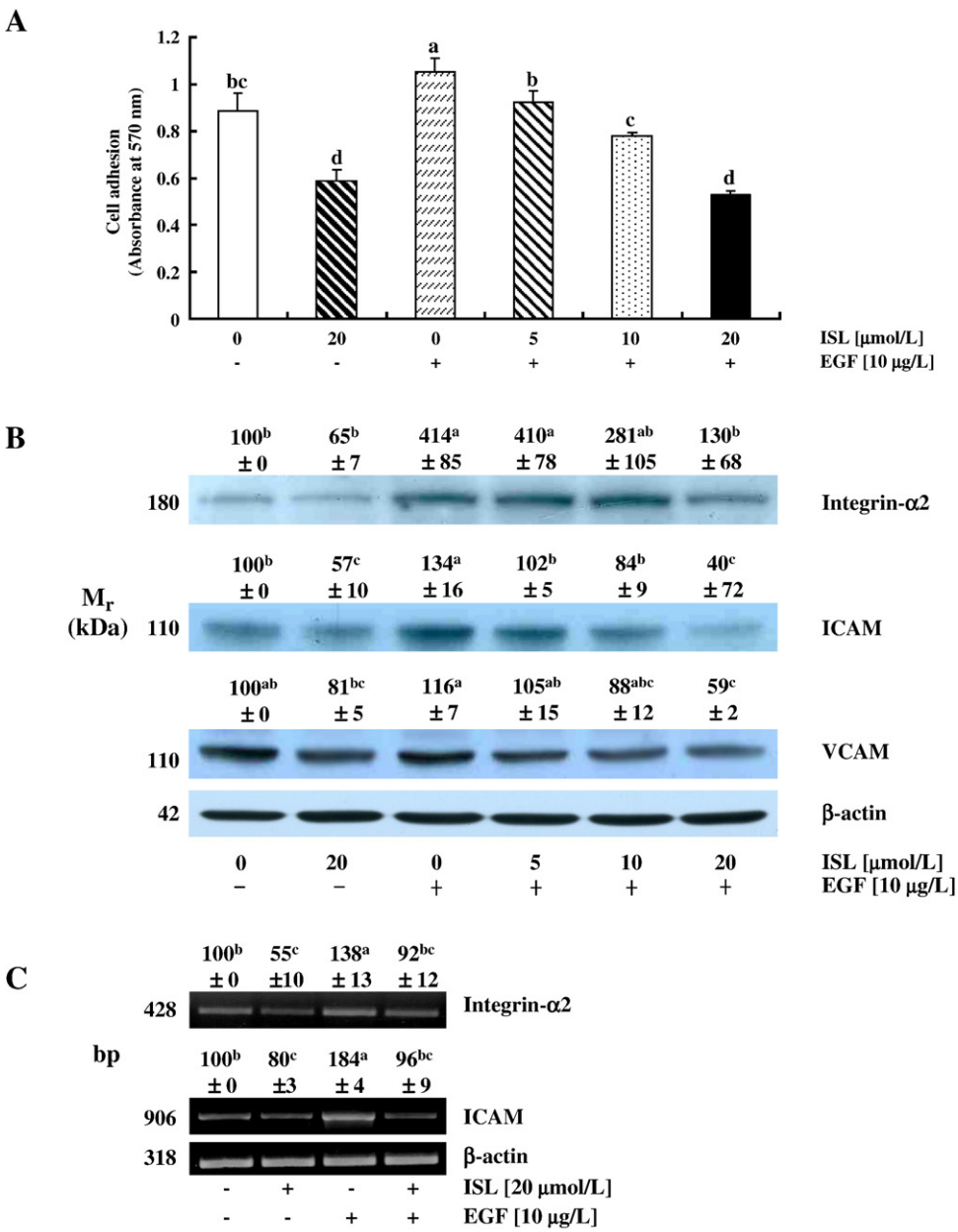

Fig. 7. ISL decreases cell adhesion of DU145 cells. (A) DU145 cells were plated in human collagen Type I-coated CytoMatrix Cell Adhesion Strips and incubated in DMEM/F12 containing 1% charcoal-stripped FBS with 0–20 μmol/L ISL in the absence or presence of 10 μg/L EGF for 45 min. Cells were stained with crystal violet, and the cell-bound stains quantified. Each bar represents the mean±S.E.M. (n=3). (B) Serum-starved DU145 cells were incubated with 0–20 μmol/L ISL in serum-free media containing 0 or 10 μg/L EGF for 48 h. Total cell lysates were prepared for immunoblotting. (C) Serum-starved cells were incubated with ISL and/or EGF for 2 h. Total RNA was isolated for RT-PCR analysis. Photographs of chemiluminescent detection of the blots (B) and ethidium bromide-stained gels (C), which are representative of three independent experiments, are shown. The relative abundance of each band to its own β-actin was quantified, and the control levels were set at 100%. The adjusted mean±S.E.M. (n=3) of each band is shown above each blot. Means without a common letter differ (P<.05).

reported. The present study demonstrates for the first time that ISL (1) inhibits migration of DU145 and LNCaP cells; (2) inhibits invasion and adhesion of DU145 cells; (3) inhibits secretion of uPA, MMP-9, TIMP-1, VEGF, integrin-α2, ICAM and VCAM; (4) stimulates TIMP-2 secretion; (5) decreases phosphorylation of Akt, JNK and c-Jun; and (6) inhibits AP-1 DNA binding activity.

One relatively frequent feature of cellular invasion mechanisms is their mediation by cell surface receptors which, in transformed cells, are often overexpressed and up-regulated. Of these receptors, the EGFR is the most frequently up-regulated in tumors including prostate cancer (reviewed in Refs. [29,30]). Aberrations in EGFR expression and downstream signaling pathways contribute to the

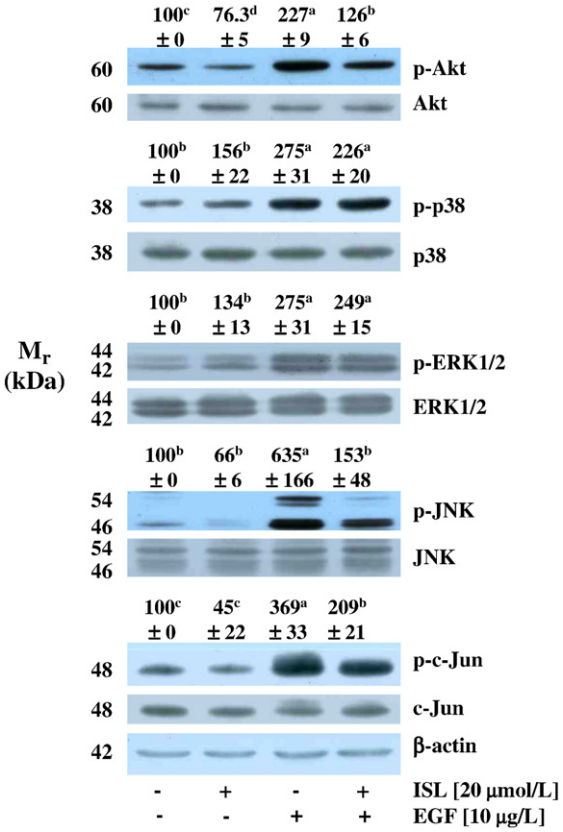

Fig. 8. ISL inhibits EGF-induced Akt and JNK signaling in DU145 cells. Serum-starved cells were incubated with 0 or 20 μmol/L ISL for 2 h and lysed without stimulation (0) or after 15 min of stimulation with EGF. Total cell lysates were subjected to immunoblotting. Photographs of chemiluminescent detection of the blots, which are representative of three independent experiments, are shown. The relative abundance of each phosphorylated band to its own control band (ratios of pAkt/Akt, p-p38/p38, p-ERK1/2/ERK1/2, p-JNK/JNK or p-c-Jun/c-Jun) was quantified, and the control levels were set at 100%. The adjusted mean±S.E.M. (n=3) of each band is shown above each blot. Means without a common letter differ (P<.05).

progression, invasion and maintenance of the malignant phenotype of many human cancers, including prostate cancer [31,32]. In addition, immunohistochemistry and microarray analyses have recently indicated that EGFR is frequently overexpressed in hormone refractory and metastatic prostate cancer [33,34]. Furthermore, clinical studies indicate that the expression of EGFR correlates with disease relapse and progression to androgen independence in human prostate cancer [31]. EGF is secreted by smooth muscle stromal cells in the human prostate [35,36] and can serve as a ligand for overexpressed EGFR in prostate cancer cells. Therefore, it is reasonable to assume that the bioactive food components that can inhibit EGFR activation could be used to inhibit prostate cancer progression. In the present study, we observed that EGF stimulated cell migration, whereas IGF-I or heregulin had no effect. In addition, EGF-induced migration, invasion and adhesion of DU145 cells and EGF-stimulated secretion of MMP-9, uPA, TIMP-1 and VEGF were suppressed by ISL, suggesting that ISL has potential as an inhibitor of prostate cancer progression.

In addition to EGF, hepatocyte growth factor/scatter factor (HGF/SF) has been reported to have the ability to induce proliferation, dissociation, migration and invasion of prostate cancer cells *in vitro* [37,38]. Furthermore, the levels of the HGF/SF receptor c-Met are elevated in prostate cancer samples, suggesting a relationship between c-Met and prostate cancer progression (reviewed in Refs. [39,40]). Future studies will be required to determine whether ISL inhibits HGF/SF-regulated pathways in prostate cancer cells.

At least three processes are necessary for cancer cell metastasis: tumor cell adhesion to the ECM, proteolytic cleavage or destruction of the ECM, and cell migration through the resultant defect. In the present study, we demonstrate that ISL decreases adhesion, invasion and migration of DU145 cells. A critical step for invasion and metastasis is the breakdown of biological barriers such as the basement membrane, which requires activation of proteolytic enzymes [41,42]. MMPs are a large family of zinc-dependent endopeptidases capable of degrading ECM components. They play an important role in tumor angiogenesis, metastasis and growth factor release from the ECM [41]. MMP-2 (72-kDa gelatinase A) and MMP-9 (92-kDa gelatinase B) seem to be involved in this initial step as they hydrolyze basal membrane Type IV collagen and have been frequently associated with the invasive metastatic potential of tumor cells, including prostate cancer [43]. uPA is a member of the serine protease family that interacts with the uPA receptor and facilitates the conversion of inactive zymogen plasminogen into broad acting serine protease plasmin [44], which plays a role in tumor invasion, tumor cell proliferation and metastasis [45]. In the present study,

Fig. 9. The JNK inhibitor SP600125 decreases cell migration and secretion of proteins related to metastasis in DU145 cells. (A) Serum-starved cells were incubated with 0 or 10 μmol/L SP600125 for 2 h and lysed without stimulation (−) or after 15 min of stimulation (+) with EGF. Total cell lysates were prepared for immunoblotting. Photographs of chemiluminescent detection of the blots, which are representative of three independent experiments, are shown. The relative abundance of each phosphorylated band to its own control band (ratios of p-JNK/JNK or p-c-Jun/c-Jun) was quantified, and the control levels were set at 100%. The adjusted mean±S.E.M. (n=3) of each band is shown above each blot. (B) Serum-starved cells were incubated with 0 or 10 μmol/L SP600125 in serum free media with or without 10 μg/L EGF. Forty-eight-hour conditioned media were collected and concentrated for Western blotting. The volumes of media loaded onto the gel were adjusted for equivalent proteins. Photographs of chemiluminescent detection of the blots, which are representative of three independent experiments, are shown. The relative abundance of each band was quantified, and the control levels were set at 100%. The adjusted mean±S.E.M. (n=3) of each band is shown above each blot. (C) The effect of EGF and/or SP600125 on the migration of DU145 cells through a Transwell filter was assessed. Each bar represents the mean±S.E.M. (n=3). (D) Cells were treated with ISL or SP600125 for 2 h and stimulated with EGF as described above. Nuclear extracts were prepared for EMSA. An autoradiography of the dried gels, which were representative of three independent experiments, is shown. The relative abundance of each band was quantified, and the control levels were set at 100%. The adjusted mean±S.E.M. (n=3) of each band is shown above each blot. Means without a common letter differ (P<.05).

EGF stimulated the secretion of MMP-9 and uPA, and ISL inhibited both basal and EGF-stimulated secretion of these proteases. These results indicate that the decreased secretion of these proteases contributes to the decrease in invasion and migration of ISL-treated DU145 cells.

Total proteolytic activity is a balance between proteases and their inhibitors. The TIMP family consists of four distinct members, of which TIMP-1 and -2 are produced by many tumor cells [46]. They bind stoichiometrically to all MMPs, but TIMP-1 preferentially inhibits MMP-9 and

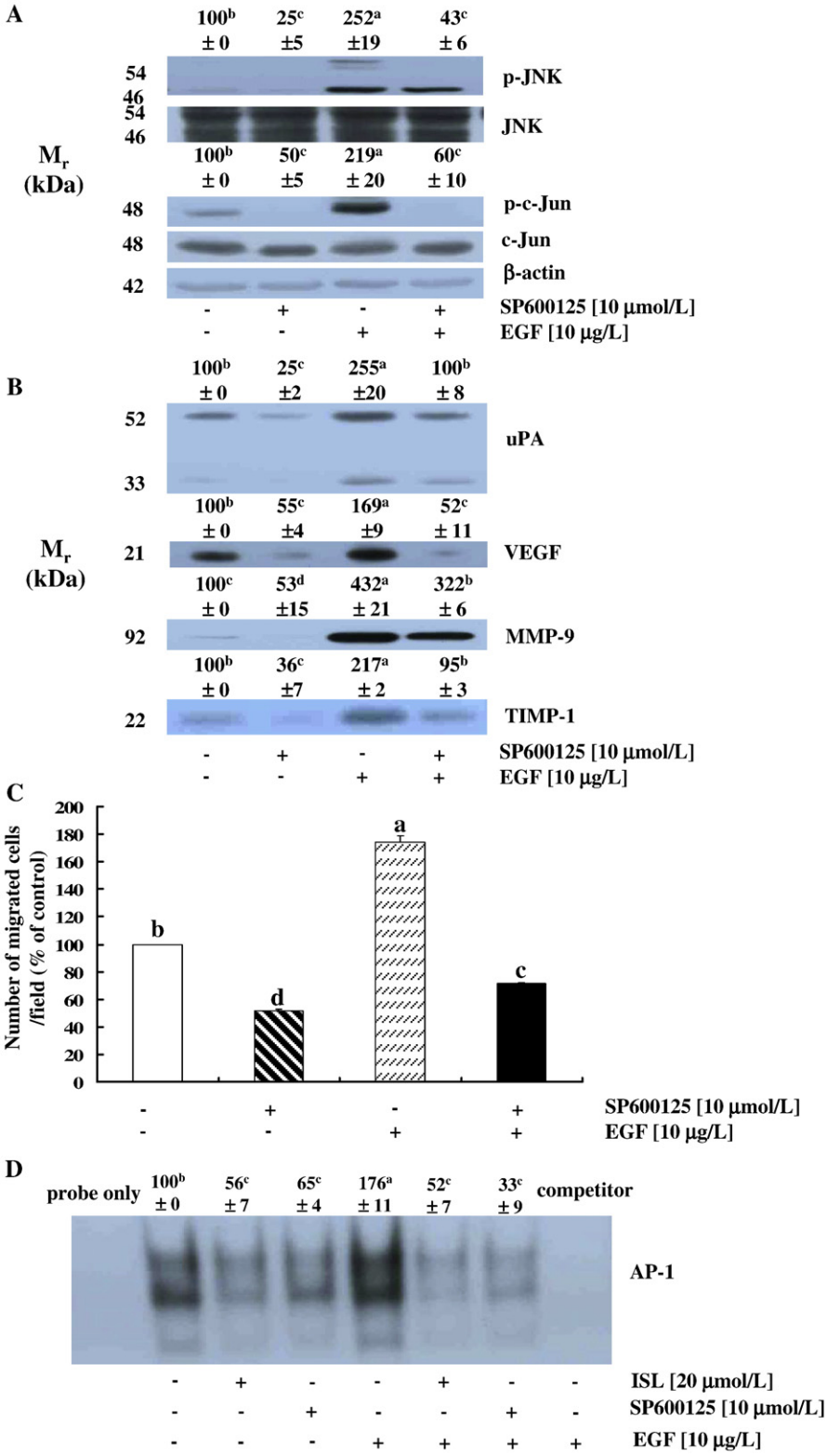

TIMP-2 preferentially inhibits MMP-2 [47,48]. Here we report that EGF stimulated TIMP-1 secretion while it was inhibited by ISL. This was an unexpected finding in view of the well-established roles of TIMP-1 in the inhibition of MMP-mediated ECM degradation, tumor cell invasion and metastasis. However, increasing evidence indicates a more complex role for TIMP-1 during tumor progression, besides its regulation of MMP-mediated ECM degradation. It has been reported that TIMP-1 mediates cell survival signal transduction pathways via its interaction with CD63/integrin-β1 complex [49]. In addition, EGF was reported to induce TIMP-1 expression and invasion of FTC-133 thyroid carcinoma cells [50]. Furthermore, high serum TIMP-1 levels were reported to correlate with poor prognosis of several types of cancer including gastric [51], colorectal [52] and breast [53] cancer. These findings suggest that TIMP-1 appears to stimulate cancer metastasis rather than suppress the process. The roles of TIMP-1 in prostate tumor cell migration and invasion remain to be determined. Both activation and activity of MMP-2 depend on TIMP-2, which plays a dual role in MMP-2 activation. In the present study, ISL increased TIMP-2 secretion, which probably contributed to the decreased invasion and migration of DU145 cells.

In order to survive and grow, a cancer cell largely depends on the support from the surrounding stromal tissue. The formation of a tumor vasculature is a crucial reaction supporting tumor growth [54], and VEGF plays a major role in tumor angiogenesis, so inhibiting VEGF production is a promising strategy for the treatment of cancer [55]. Here we demonstrate that ISL inhibits VEGF production in DU145 cells. It remains to be determined whether ISL inhibits VEGF synthesis thereby reducing angiogenesis *in vivo*. In addition to promoting angiogenesis, it has been shown that VEGF acts directly on prostate cancer cells *in vitro*, suggesting that VEGF may be more than an angiogenic factor in the prostate [56].

We observed that ISL inhibits cell adhesion, which was related to decreases in integrin-α2, ICAM and VCAM (Fig. 7). The present results indicate that decreases in these adhesion-regulating molecules contribute to ISL-induced decreases in DU145 cell adhesion. Integrins are noncovalently associated, heterodimeric cell surface glycoproteins with α- and β-subunits. Integrins mediate adhesion between cells and their neighboring matrices and transmit important signals regulating cell survival, differentiation and migration [57]. Most integrins activate MAPK and PI3K, leading to activation of Akt [57]. In the present study, ISL also decreased phosphorylation of Akt and JNK. Future studies are needed to explore the relationship between expression of integrin-α2 and phosphorylation of Akt and JNK in ISL-treated prostate cancer cells.

JNKs are able to phosphorylate and to activate several transcription factors including c-Jun, which is a part of the transcription factor AP-1. AP-1 controls the transcription of many genes including VEGF [58], MMP-9 [59], uPA [60], integrin-α [61] and ICAM [62]. In the present study, we observed that ISL inhibited not only EGF-induced phosphorylation of JNK and c-Jun, but also EGF-induced VEGF, MMP-9 and uPA expression, suggesting that inhibition of AP-1 activity (inhibition of JNK/c-Jun activation) by ISL is involved in the inhibition of VEGF, MMP-9 and uPA expression. In addition, suppression of JNK activity by SP600125 inhibited both basal and EGF-induced expression of uPA, VEGF, MMP-9 and TIMP-1 (Fig. 9B). Furthermore, the JNK inhibitor significantly inhibited both basal and EGF-induced migration of DU145 cells (Fig. 9C). These results indicate that inhibition of JNK activity contributes to the decrease in migration of ISL-treated DU145 cells.

The present results suggest that ISL may have efficacy, if delivered to the prostate at concentrations between 5 and 20 μmol/L, in preventing the metastasis of prostate cancer. Previous work with intestinal epithelial cell line-6 [14] and the present results with PWR-1E normal prostate epithelial cells indicate that ISL at the concentrations used in the present study is not toxic to normal cells. With CT-29 colon cancer cells inoculated in syngeneic BALB/c mice, we have shown that ISL (1 mg/kg body weight) reduced tumor sizes without any detectable nephrotoxicity or hepatoxicity. In fact, ISL suppressed cisplatin-induced kidney and liver damage [63]. To the best of our knowledge, no data have yet been published regarding the ISL concentrations in human blood. These data together with published results demonstrating the efficacy of ISL in inhibiting chemically induced colonic tumorigenesis [12], skin papilloma formation [11] and lung metastasis of murine renal cell carcinoma cells [13] indicate that further evaluation of the potential of ISL as a chemopreventive agent in human clinical studies is warranted.

In conclusion, the present study assessed the efficacy of ISL anti-metastasis and identified the associated mechanisms in both androgen-dependent and androgen-independent human prostate cancer cells. Future in vivo efficacy studies with ISL in preclinical prostate cancer models are indicated. Prostate tumor invasion and metastasis present major obstacles to successful cancer control. In addition, androgen-resistant prostate cancer does not respond well to cytotoxic agents and has a high mortality rate. Thus, inhibition of metastasis of androgen-independent prostate cancer cells by ISL could have important preventive and therapeutic benefits.

References

[1] Surh YJ. Cancer chemoprevention with dietary phytochemicals. Nat Rev Cancer 2003;3:768–80.
[2] Sporn MB, Suh N. Chemoprevention of cancer. Carcinogenesis 2000;21:525–30.
[3] Lippman SM, Hong WK. Cancer prevention science and practice. Cancer Res 2002;62:5119–25.
[4] Clinton SK, Giovannucci E. Diet, nutrition, and prostate cancer. Annu Rev Nutr 1998;18:413–40.

[5] Kelloff GJ. Perspectives on cancer chemoprevention research and drug development. Adv Cancer Res 2000;78:199–334.
[6] Jemal A, Siegel R, Ward E, Murray T, Xu J, Thun MJ. Cancer statistics, 2007. CA Cancer J Clin 2007;57:43–66.
[7] Sporn MB. The war on cancer. Lancet 1996;347:1377–81.
[8] Kelloff GJ, Lieberman R, Steele VE, Boone CW, Lubet RA, Kopelovitch L, et al. Chemoprevention of prostate cancer: concepts and strategies. Eur Urol 1999;35:342–50.
[9] Kim EJ, Park SY, Shin HK, Kwon DY, Surh YJ, Park JH. Activation of caspase-8 contributes to 3,3¢-diindolylmethane-induced apoptosis in colon cancer cells. J Nutr 2007;137:31–6.
[10] Singh RP, Agarwal R. Prostate cancer chemoprevention by silibinin: bench to bedside. Mol Carcinog 2006;45:436–42.
[11] Yamamoto S, Aizu E, Jiang H, Nakadate T, Kiyoto I, Wang JC, et al. The potent anti-tumor-promoting agent isoliquiritigenin. Carcinogenesis 1991;12:317–23.
[12] Baba M, Asano R, Takigami I, Takahashi T, Ohmura M, Okada Y, et al. Studies on cancer chemoprevention by traditional folk medicines: XXV. Inhibitory effect of isoliquiritigenin on azoxymethane-induced murine colon aberrant crypt focus formation and carcinogenesis. Biol Pharm Bull 2002;25:247–50.
[13] Yamazaki S, Morita T, Endo H, Hamamoto T, Baba M, Joichi Y, et al. Isoliquiritigenin suppresses pulmonary metastasis of mouse renal cell carcinoma. Cancer Lett 2002;183:23–30.
[14] Jung JI, Lim SS, Choi HJ, Cho HJ, Shin HK, Kim EJ, et al. Isoliquiritigenin induces apoptosis by depolarizing mitochondrial membranes in prostate cancer cells. J Nutr Biochem 2006;17:689–96.
[15] Kanazawa M, Satomi Y, Mizutani Y, Ukimura O, Kawauchi A, Sakai T, et al. Isoliquiritigenin inhibits the growth of prostate cancer. Eur Urol 2003;43:580–6.
[16] Jung JI, Chung E, Seon MR, Shin HK, Kim EJ, Lim SS, et al. Isoliquiritigenin (ISL) inhibits ErbB3 signaling in prostate cancer cells. Biofactors 2006;28:159–68.
[17] Bennett BL, Sasaki DT, Murray BW, O'Leary EC, Sakata ST, Xu W, et al. SP600125, an anthrapyrazolone inhibitor of Jun N-terminal kinase. Proc Natl Acad Sci U S A 2001;98:13681–6.
[18] Kim EJ, Holthuizen PE, Park HS, Ha YL, Jung KC, Park JHY. *Trans*-10,*cis*-12 conjugated linoleic acid inhibits Caco-2 colon cancer cell growth. Am J Physiol Gastrointest Liver Physiol 2002;283:G357–67.
[19] Cho HJ, Kim WK, Kim EJ, Jung KC, Park S, Lee HS, et al. Conjugated linoleic acid inhibits cell proliferation and ErbB3 signaling in HT-29 human colon cell line. Am J Physiol Gastrointest Liver Physiol 2003;284:G996–G1005.
[20] Kim EJ, Kang IJ, Cho HJ, Kim WK, Ha YL, Park JH. Conjugated linoleic acid downregulates insulin-like growth factor-I receptor levels in HT-29 human colon cancer cells. J Nutr 2003;133:2675–81.
[21] Lim DY, Tyner AL, Park JB, Lee JY, Choi YH, Park JH. Inhibition of colon cancer cell proliferation by the dietary compound conjugated linoleic acid is mediated by the CDK inhibitor p21(CIP1/WAF1). J Cell Physiol 2005;205:107–13.
[22] Culig Z, Hobisch A, Cronauer MV, Radmayr C, Trapman J, Hittmair A, et al. Androgen receptor activation in prostatic tumor cell lines by insulin-like growth factor-I, keratinocyte growth factor, and epidermal growth factor. Cancer Res 1994;54:5474–8.
[23] Cha HJ, Bae SK, Lee HY, Lee OH, Sato H, Seiki M, et al. Anti-invasive activity of ursolic acid correlates with the reduced expression of matrix metalloproteinase-9 (MMP-9) in HT1080 human fibrosarcoma cells. Cancer Res 1996;56:2281–4.
[24] Strongin AY, Marmer BL, Grant GA, Goldberg GI. Plasma membrane-dependent activation of the 72-kDa type IV collagenase is prevented by complex formation with TIMP-2. J Biol Chem 1993;268:14033–9.
[25] Hackel PO, Zwick E, Prenzel N, Ullrich A. Epidermal growth factor receptors: critical mediators of multiple receptor pathways. Curr Opin Cell Biol 1999;11:184–9.
[26] Iwashita K, Kobori M, Yamaki K, Tsushida T. Flavonoids inhibit cell growth and induce apoptosis in B16 melanoma 4A5 cells. Biosci Biotechnol Biochem 2000;64:1813–20.
[27] Maggiolini M, Statti G, Vivacqua A, Gabriele S, Rago V, Loizzo M, et al. Estrogenic and antiproliferative activities of isoliquiritigenin in MCF7 breast cancer cells. J Steroid Biochem Mol Biol 2002;82: 315–22.
[28] Ma J, Fu NY, Pang DB, Wu WY, Xu AL. Apoptosis induced by isoliquiritigenin in human gastric cancer MGC-803 cells. Planta Med 2001;67:754–7.
[29] Wells A. Tumor invasion: role of growth factor-induced cell motility. Adv Cancer Res 2000;78:31–101.
[30] Kim HG, Kassis J, Souto JC, Turner T, Wells A. EGF receptor signaling in prostate morphogenesis and tumorigenesis. Histol Histopathol 1999;14:1175–82.
[31] Di Lorenzo G, Tortora G, D'Armiento FP, De Rosa G, Staibano S, Autorino R, et al. Expression of epidermal growth factor receptor correlates with disease relapse and progression to androgen-independence in human prostate cancer. Clin Cancer Res 2002;8:3438–44.
[32] Hegeman RB, Liu G, Wilding G, McNeel DG. Newer therapies in advanced prostate cancer. Clin Prostate Cancer 2004;3:150–6.
[33] Hernes E, Fossa SD, Berner A, Otnes B, Nesland JM. Expression of the epidermal growth factor receptor family in prostate carcinoma before and during androgen-independence. Br J Cancer 2004;90: 449–54.
[34] Zellweger T, Ninck C, Bloch M, Mirlacher M, Koivisto PA, Helin HJ, et al. Expression patterns of potential therapeutic targets in prostate cancer. Int J Cancer 2005;113:619–28.
[35] Rajan R, Vanderslice R, Kapur S, Lynch J, Thompson R, Djakiew D. Epidermal growth factor (EGF) promotes chemomigration of a human prostate tumor cell line, and EGF immunoreactive proteins are present at sites of metastasis in the stroma of lymph nodes and medullary bone. Prostate 1996;28:1–9.
[36] Freeman MR, Paul S, Kaefer M, Ishikawa M, Adam RM, Renshaw AA, et al. Heparin-binding EGF-like growth factor in the human prostate: synthesis predominantly by interstitial and vascular smooth muscle cells and action as a carcinoma cell mitogen. J Cell Biochem 1998;68:328–38.
[37] Gmyrek GA, Walburg M, Webb CP, Yu HM, You X, Vaughan ED, et al. Normal and malignant prostate epithelial cells differ in their response to hepatocyte growth factor/scatter factor. Am J Pathol 2001;159:579–90.
[38] Fujiuchi Y, Nagakawa O, Murakami K, Fuse H, Saiki I. Effect of hepatocyte growth factor on invasion of prostate cancer cell lines. Oncol Rep 2003;10:1001–6.
[39] Hurle RA, Davies G, Parr C, Mason MD, Jenkins SA, Kynaston HG, et al. Hepatocyte growth factor/scatter factor and prostate cancer: a review. Histol Histopathol 2005;20:1339–49.
[40] Knudsen BS, Edlund M. Prostate cancer and the met hepatocyte growth factor receptor. Adv Cancer Res 2004;91:31–67.
[41] Coussens LM, Werb Z. Matrix metalloproteinases and the development of cancer. Chem Biol 1996;3:895–904.
[42] Liotta LA, Stetler-Stevenson WG. Tumor invasion and metastasis: an imbalance of positive and negative regulation. Cancer Res 1991;51: 5054s–9s.
[43] Zhang L, Shi J, Feng J, Klocker H, Lee C, Zhang J. Type IV collagenase (matrix metalloproteinase-2 and -9) in prostate cancer. Prostate Cancer Prostatic Dis 2004;7:327–32.
[44] Castellino FJ, Ploplis VA. Structure and function of the plasminogen/plasmin system. Thromb Haemost 2005;93:647–54.
[45] Kwaan HC. The plasminogen–plasmin system in malignancy. Cancer Metastasis Rev 1992;11:291–311.
[46] Brew K, Dinakarpandian D, Nagase H. Tissue inhibitors of metalloproteinases: evolution, structure and function. Biochim Biophys Acta 2000;1477:267–83.
[47] Wilhelm SM, Collier IE, Marmer BL, Eisen AZ, Grant GA, Goldberg GI. SV40-transformed human lung fibroblasts secrete a 92-kDa type IV collagenase which is identical to that secreted by normal human macrophages. J Biol Chem 1989;264:17213–21.
[48] Stetler-Stevenson WG, Krutzsch HC, Liotta LA. Tissue inhibitor of

metalloproteinase (TIMP-2). A new member of the metalloproteinase inhibitor family. J Biol Chem 1989;264:17374–8.
[49] Chirco R, Liu XW, Jung KK, Kim HR. Novel functions of TIMPs in cell signaling. Cancer Metastasis Rev 2006;25:99–113.
[50] Soula-Rothhut M, Coissard C, Sartelet H, Boudot C, Bellon G, Martiny L, et al. The tumor suppressor PTEN inhibits EGF-induced TSP-1 and TIMP-1 expression in FTC-133 thyroid carcinoma cells. Exp Cell Res 2005;304:187–201.
[51] Joo YE, Seo KS, Kim HS, Rew JS, Park CS, Kim SJ. Expression of tissue inhibitors of metalloproteinases (TIMPs) in gastric cancer. Dig Dis Sci 2000;45:114–21.
[52] Zeng ZS, Cohen AM, Zhang ZF, Stetler-Stevenson W, Guillem JG. Elevated tissue inhibitor of metalloproteinase 1 RNA in colorectal cancer stroma correlates with lymph node and distant metastases. Clin Cancer Res 1995;1:899–906.
[53] Wu ZS, Wu Q, Yang JH, Wang HQ, Ding XD, Yang F, et al. Prognostic significance of MMP-9 and TIMP-1 serum and tissue expression in breast cancer. Int J Cancer 2008;122:2050–6.
[54] Folkman J. Role of angiogenesis in tumor growth and metastasis. Semin Oncol 2002;29:15–8.
[55] Ferrara N, Kerbel RS. Angiogenesis as a therapeutic target. Nature 2005;438:967–74.
[56] Chevalier S, Defoy I, Lacoste J, Hamel L, Guy L, Begin LR, et al. Vascular endothelial growth factor and signaling in the prostate: more than angiogenesis. Mol Cell Endocrinol 2002;189:169–79.
[57] Eccles SA. Parallels in invasion and angiogenesis provide pivotal points for therapeutic intervention. Int J Dev Biol 2004;48:583–98.
[58] Finkenzeller G, Technau A, Marme D. Hypoxia-induced transcription of the vascular endothelial growth factor gene is independent of functional AP-1 transcription factor. Biochem Biophys Res Commun 1995;208:432–9.
[59] Cho HJ, Kang JH, Kwak JY, Lee TS, Lee IS, Park NG, et al. Ascofuranone suppresses PMA-mediated matrix metalloproteinase-9 gene activation through the Ras/Raf/MEK/ERK- and Ap1-dependent mechanisms. Carcinogenesis 2007;28:1104–10.
[60] De Cesare D, Vallone D, Caracciolo A, Sassone-Corsi P, Nerlov C, Verde P. Heterodimerization of c-Jun with ATF-2 and c-Fos is required for positive and negative regulation of the human urokinase enhancer. Oncogene 1995;11:365–76.
[61] Zutter MM, Santoro SA, Painter AS, Tsung YL, Gafford A. The human alpha 2 integrin gene promoter. Identification of positive and negative regulatory elements important for cell-type and developmentally restricted gene expression. J Biol Chem 1994;269:463–9.
[62] Tsou TC, Yeh SC, Tsai FY, Chen JW, Chiang HC. Glutathione regulation of redox-sensitive signals in tumor necrosis factor-alpha-induced vascular endothelial dysfunction. Toxicol Appl Pharmacol 2007;221:168–78.
[63] Lee CK, Son SH, Park KK, Park JH, Lim SS, Chung WY. Isoliquiritigenin inhibits tumor growth and protects the kidney and liver against chemotherapy-induced toxicity in a mouse xenograft model of colon carcinoma. J Pharmacol Sci 2008;106:444–51.